

# Microneedle-Mediated Delivery of Atenolol and Bisoprolol Hemifumarate

Kevin Ita<sup>1,\*</sup>, Nanik Hatsakorzian<sup>1</sup>, and Vladimir Tolstikov<sup>2,†</sup>

<sup>1</sup> College of Pharmacy, Touro University, Mare Island-Vallejo, California, 94592, USA

<sup>2</sup> Metabolomics Core Facility, Genome Center, University of California, Davis, California, 95616, USA

In the present study, silicon, stainless steel microneedles as well as gold-titanium microneedle roller were used to deliver atenolol and bisoprolol transdermally. *In vitro* permeation studies were carried out at 37° across porcine ear skin. A vertical, three-compartment flow-through diffusion cell system was used for experiments. The amounts of atenolol and bisoprolol hemifumarate that permeated into the receptor compartment were analyzed using liquid chromatography-mass spectrometry. Passive flux for atenolol was 1.18 ng/cm<sup>2</sup>/hr. Transcutaneous flux values following the use of silicon and stainless steel microneedles were 2.35- and 2.62 ng/cm<sup>2</sup>/hr respectively. Twelve passes of a gold-titanium microneedle roller resulted in a transdermal flux of 1.65 ng/cm<sup>2</sup>/hr for atenolol. Passive transcutaneous flux for bisoprolol was 1.17 μg/cm<sup>2</sup>/hr. Transcutaneous flux values for bisoprolol following the use of silicon and stainless steel microneedles were 2.79- and 2.31 μg/cm<sup>2</sup>/hr respectively. For bisoprolol hemifumarate, twelve passes of a gold-titanium microneedle skin roller resulted in a transdermal flux of 3.44 μg/cm<sup>2</sup>/hr. In conclusion, microneedles significantly enhanced the percutaneous penetration of atenolol and bisoprolol. It may be feasible to develop transdermal microneedle patches for these drugs.

**KEYWORDS:** Transdermal Drug Delivery, Atenolol, Bisoprolol, Microneedles.

## INTRODUCTION

Hypertension is the leading risk factor for mortality and is ranked third as a cause of disability-adjusted life-years.<sup>1</sup> According to the World Health Organization (WHO), global figures for the disease may be as high as 1 billion. About 7.1 million deaths per year is attributable to hypertension. WHO reports that high blood pressure (>115 mmHg systolic blood pressure) is responsible for 62% of cerebrovascular disease and 49 percent of ischemic heart disease.<sup>2</sup> Uncontrolled high blood pressure also increases the risk of congestive heart failure, chronic renal insufficiency, stroke and coronary artery disease.<sup>3</sup>

Most antihypertensive medications are oral and possess low bioavailability. Because patients have to take some these tablets many times daily, there is also the problem of low compliance. Transdermal delivery offers

the significant advantage of administering drugs non-invasively. As the largest organ of the human body, the skin also provides a painless and accessible interface for systemic drug administration<sup>4</sup> which normally improves patient compliance relative to oral delivery requiring multiple doses each day. In addition there is convenience, elimination of first-pass effect and provision of stable plasma drug concentration.<sup>5–7</sup>

The principal disadvantage is that stratum corneum limits the number of drugs that can cross into the bloodstream in therapeutic concentrations.

Several approaches have been developed to overcome the stratum corneum barrier including safe laser technology,<sup>8</sup> sonophoresis,<sup>9,10</sup> iontophoresis<sup>11,12</sup> and the use of chemical penetration enhancers.<sup>13</sup> One of the methods used to bypass the skin barrier is microneedle arrays.<sup>14,15</sup> Microneedles are long enough to penetrate the stratum corneum but short enough to avoid the nerves located in the dermis, potentially offering the prospect of minimally invasive but painless drug delivery.<sup>16</sup> Microneedle arrays can disrupt the stratum corneum in a pain-free and efficient manner.<sup>17</sup> The major advantage of microneedles is that they can provide a painless means

\* Author to whom correspondence should be addressed.

Email: kevin.ita@tu.edu

† Present address: Translational Sciences, Eli Lilly and Company, Lilly Corporate Center, Indianapolis, 46285 IN, USA.

Received: 17 September 2012

Accepted: 18 February 2013

of transporting molecules into and through the skin. Most research projects to date have focused on making microscopic holes in the skin by inserting solid microneedles made from steel or silicon. The 'poke with patch' approach uses microneedles to make holes before applying a transdermal patch.<sup>18,19</sup>

Atenolol and bisoprolol are  $\beta$ -blocking agents used in the management of hypertension. These drugs are hydrophilic with log *P* values of  $-1.4$  and  $-0.05$  respectively.<sup>20,21</sup> Puglia and Bonina<sup>22</sup> have evaluated percutaneous absorption of atenolol as a candidate for transdermal drug delivery. Zhao et al.<sup>23</sup> have also studied bisoprolol as a transdermal drug delivery candidate. Due to low partition coefficients, passive penetration of these drugs across the skin is low. Facilitated transdermal delivery of these drugs would be beneficial for hypertensive patients. The aim of this paper was to study the influence of microneedles on transdermal delivery of atenolol and bisoprolol across porcine ear skin *in vitro*.

## MATERIALS AND METHODS

### Materials and Apparatus

500  $\mu\text{m}$  silicon microneedles were made by laser micro-machining (Laserod, Torrance, CA). Also, 500  $\mu\text{m}$  stainless steel microneedles (Adminpatch) were purchased from NanoBioSciences, Sunnyvale, CA. This patented device made from SS316 stainless steel has 187 microneedles on 1  $\text{cm}^2$  circular microneedle array. The third means of microporation was with a microneedle skin roller (New Skin Care Collection, Talahassee, Florida, USA). This stainless steel roller unit has 200  $\mu\text{m}$  needles protruding from a cylindrical assembly containing 24 circular arrays of 8 needles each (192 needles in total). Digital images of microneedles were taken with a Samsung HTC digital camera. Atenolol and bisoprolol hemifumarate were purchased from Sigma Aldrich (St Louis, MO, USA). Demineralized water was used throughout the study. LC-MS grade acetonitrile was purchased from Burdick and Jackson (VWR International, West Chester, PA, USA). Extra pure formic acid was purchased from EMD (Gibbstown, NJ, USA). The ultrapure water was supplied by an in-house Millipore system (Billerica, MA, USA). Fresh aqueous buffers for LC-MS analysis were prepared on the working day.

### Liquid Chromatography-Tandem Mass Spectrometry

Liquid chromatography-tandem mass spectrometry was performed with Waters Acquity UPLC system (Waters Corp., Milford, MA, USA) interfaced to an Applied Biosystems Sciex 4000-QTRAP mass spectrometer (Applied Biosystems, Foster City, CA, USA). Analyst software (Version 1.42) was used for data acquisition and processing. Separations were carried out on a UPLC HSS T3  $\text{C}_{18}$  column  $2.1 \times 50$  mm equipped with HSS T3

$\text{C}_{18}$  pre-column (Waters Corp., Milford, MA, USA). The mobile phase was 0.1% formic acid in water and 0.1% formic acid in acetonitrile. The flow rate was 0.6 ml/min. Injection volume was 2  $\mu\text{l}$ . Injection mode was partial loop with the needle overfill. Weak wash solvent was water. Strong wash solvent was acetonitrile. The retention time was 1.47 min. Detection was performed on a QTRAP 4000 LC-MS/MS system equipped with Turbolon electrospray ion source. The LC-MS/MS detector was operated using multiple reaction monitoring (MRM) mode. MRM transition was predetermined for atenolol: Q1 267.00 (parent ion  $[\text{M}+\text{H}]^+$ ) and Q3 144.9 (daughter ion  $[\text{M}+\text{H}]^+$ ). The corresponding values for bisoprolol were Q1 326.00 (parent ion  $[\text{M}+\text{H}]^+$ ) and Q3 116.00 (daughter ion  $[\text{M}+\text{H}]^+$ ). Turbo spray ion source settings were as follows—curtain gas, gas 1 and gas 2 (nitrogen) 20, 50 and 50 psi respectively; collision activated dissociation (CAD) gas: high. The dwell time was 100 ms while source temperature and ion spray voltage were 500  $^{\circ}\text{C}$  and 1500 V respectively. Declustering potential (DP) and collision energy (CE) were 50 V and 23 eV respectively. Collision extraction potential was set at 20 V. The analytical range to be validated was chosen on the basis of expected percutaneous concentrations. The lower limit of quantitation was 1 ng/ml.

### Pig Ear Skin Preparation

Institutional Animal Care and Use Committee (IACUC) and Institutional Biosafety Committee (IBC) of Touro University, Mare Island-Vallejo, California approved the experiments. Pig ear skin was obtained from a local slaughter house and cleaned under water. The whole skin was removed from the outer region of the ear and separated from the underlying cartilage. Skin pieces were maintained at  $-20$   $^{\circ}\text{C}$  for no longer than one month. Just prior to experiments, the skin was thawed at room temperature over a one hour period.

### In Vitro Skin Penetration Experiments

A vertical, three compartments, flow-through diffusion cell system (LG-1088-IC, Laboratory Glass Apparatus, Inc., Berkeley) was used for experiments. Exposed skin area was 0.8  $\text{cm}^2$ . After equilibration, the donor compartment of each cell was charged with 27 mg/ml of atenolol. The donor compartment was covered with parafilm. The physiological receiver solution was phosphate buffered saline (pH 7.4). Diffusion cells were kept at 37  $^{\circ}\text{C}$  by Digital One heating bath circulator (Neslab EX-7, Thermo Fisher, USA) and stirred at 100 rpm (Variomag, Daytona Beach, FL, USA). Percutaneous transport was monitored for 12 hours. The receptor was constantly perfused at 3 ml/min using a peristaltic pump (Ismatec ISM 943) and samples were collected in two-hour increments using a fraction collector (Retriever 500, Teledyne Isco, USA).

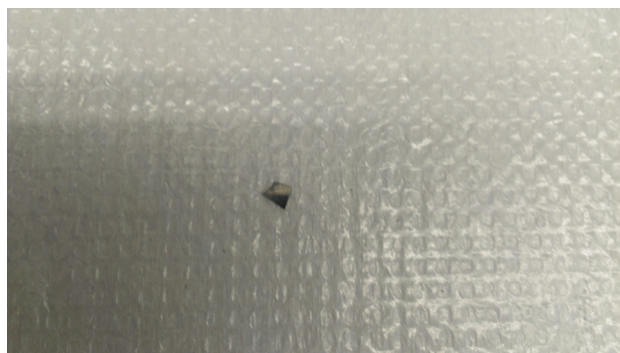


**Figure 1.** Silicon microneedle.

The cumulative quantity of atenolol transported was determined using liquid chromatography-tandem mass spectrometry (LC-MS/MS) as described above.

### Microneedle-Mediated Transdermal Delivery

Silicon (Fig. 1), stainless steel (Fig. 2) microneedles as well as gold-titanium microneedle roller (Fig. 3) were used for the experiments. Both silicon and stainless steel microneedles were manually pressed into excised pig ear skin. Treated skin was then clamped between donor and receptor compartments of the diffusion cell. Microneedle skin rollers were rolled diagonally across pig ear skin surface twelve times. All *in vitro* skin penetration experiments were then performed as described earlier.

### Data Analysis

Cumulative amounts of atenolol and bisoprolol (Figs. 4(a and b)) in the receiver compartment were plotted as a function of time. Flux was calculated from the concentrations in the collecting tubes by using the equation

$$J_F = F \cdot C_a / A \quad (1)$$

where  $J_F$  is the flux through porcine skin,  $C_a$  is the concentration of the permeant in the receptor phase,  $A$  is the skin area and  $F$  is the flow rate of phosphate buffered saline.

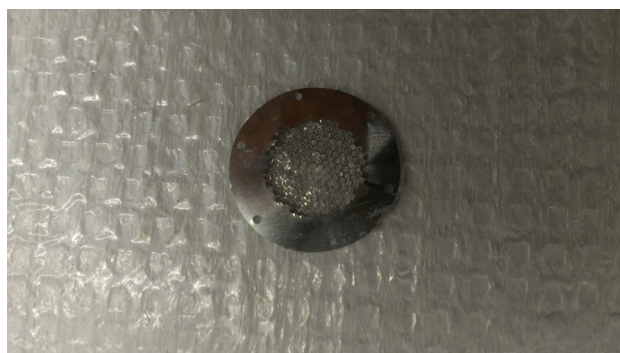


**Figure 2.** Stainless steel microneedles.



**Figure 3.** Gold-titanium microneedle roller.

Steady-state fluxes of atenolol and bisoprolol were calculated by linear regression from the steady-state portion of the cumulative amount versus time curves.

### Statistical Analysis

Statistical analysis of data was carried out by one-way ANOVA. A  $p$  value of  $<0.05$  was considered statistically significant.

## RESULTS

### LC-MS/MS

LC-MS/MS method was developed for monitoring atenolol and bisoprolol following transdermal administration. The detector was operated using multiple reaction monitoring (MRM) mode. MRM transition was predetermined for atenolol: Q1 267.00 (parent ion  $[M+H]^+$ ) and Q3 144.9 (daughter ion  $[M+H]^+$ ) and bisoprolol: Q1 326.00 (parent

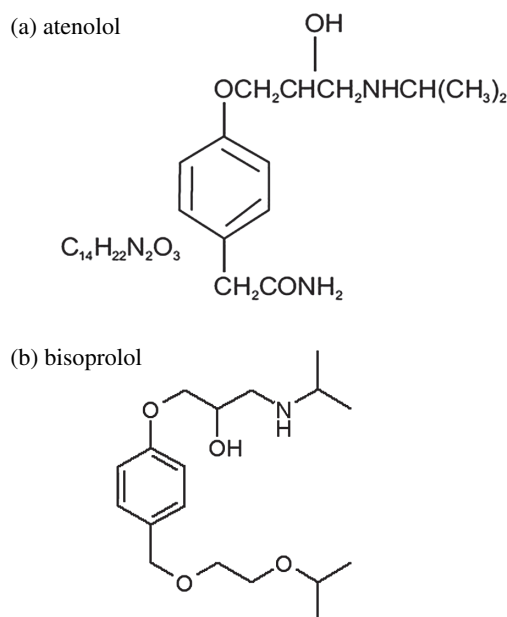


**Figure 4.** Molecular structures of atenolol (a) and bisoprolol (b).

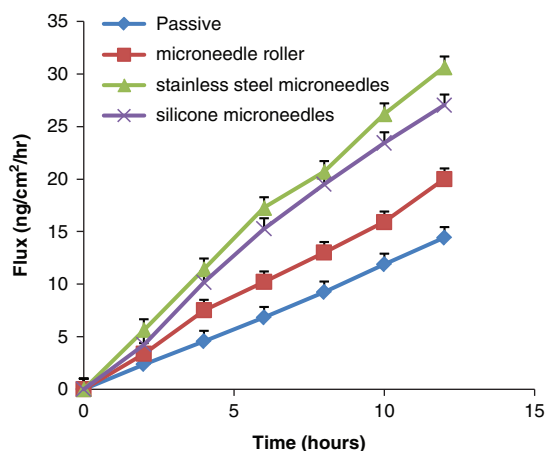


**Figure 5.** The effect of microneedles on percutaneous penetration of atenolol across porcine skin.

ion  $[M+H]^+$  and Q3 116.00 (daughter ion  $[M+H]^+$ ) respectively. Chromatographic conditions were investigated to optimize sensitivity, speed and peak shape. Rapid separation was achieved. Addition of an acidic modifier (formic acid) to the mobile phase improved sensitivity. The mobile phase used in this experiment (acetonitrile, water and formic acid) provided symmetrical peak shapes. The present LC-MS/MS method offered a limit of quantitation of 1 ng/ml.

### In Vitro Skin Penetration Experiments

We carried out skin permeation studies to quantify the influence of microneedles on transdermal delivery of two hydrophilic permeants- atenolol and bisoprolol. Pig ear skin was used since it is a representative model of human epidermal membrane. This has been previously alluded to by some investigators.<sup>24, 25</sup> Pig ear skin was clamped between two compartments, a donor, which contains the drug solution at a certain concentration and a receptor

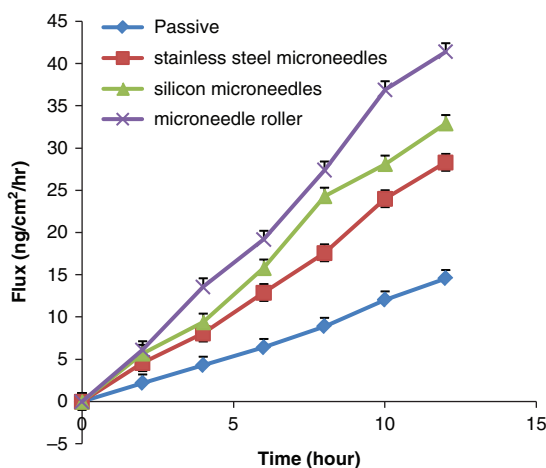


**Figure 6.** Percutaneous penetration of bisoprolol hemifumarate from microneedles.

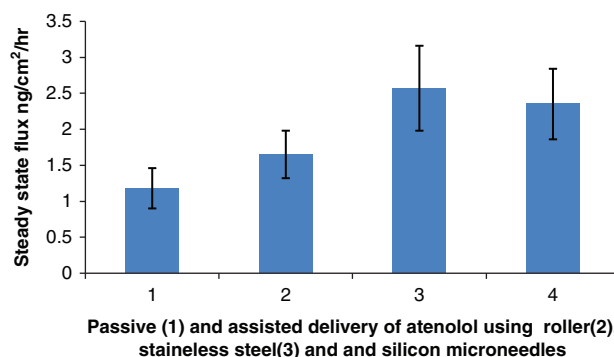


**Figure 7.** Passive and assisted delivery of atenolol using roller (2), stainless steel (3) and silicon microneedles.

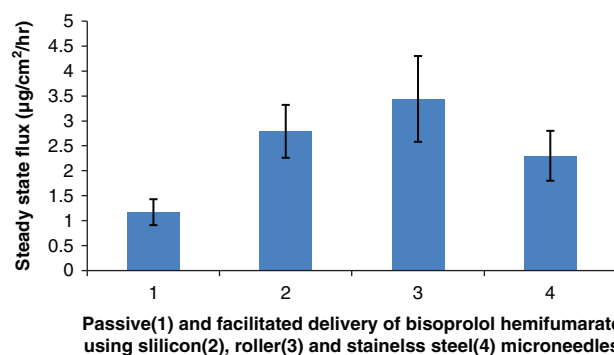


**Figure 8.** Transdermal delivery of bisoprolol hemifumarate using roller (2), stainless steel (3) and silicon microneedles.

compartment, where solution concentration is assumed to be zero.<sup>26</sup>

At steady-state, flux is

$$J_{ss} = DC_{ss}/h \quad (2)$$

$$\text{and lag time } t_{lag} = h^2/6D \quad (3)$$

where  $D$  is diffusion coefficient,  $C$ -concentration and  $h$ -membrane thickness. In Eq. (3),  $t_{lag}$  is lag time. Flux values were determined for both atenolol and bisoprolol from the steady-state portion of the cumulative amount versus time curves. Passive penetration rates of atenolol and bisoprolol across porcine ear skin were low. Cumulative amount versus time curves for atenolol and bisoprolol hemifumarate are shown in Figures 5 and 6. The corresponding bar plots are illustrated in Figures 7 and 8. Flux values for atenolol and bisoprolol are shown in Tables I

**Table I.** Effect of microneedles on transdermal delivery of atenolol.

	Flux (ng/cm²/hr)
Passive delivery	1.18 ± 0.28
Stainless steel microneedles	2.62 ± 0.59
Silicon microneedles	2.35 ± 0.49
Microneedle roller	1.65 ± 0.33



**Table II.** Microneedle-assisted transcutaneous flux of bisoprolol hemifumarate.

	Flux ( $\mu\text{g}/\text{cm}^2/\text{hr}$ )
Passive delivery	$1.17 \pm 0.26$
Stainless steel microneedles	$2.3 \pm 0.50$
Silicon microneedles	$2.79 \pm 0.53$
Microneedle roller	$3.44 \pm 0.86$

and II. Passive flux values for atenolol and bisoprolol were  $1.18 \text{ ng}/\text{cm}^2/\text{hr}$  and  $1.17 \mu\text{g}/\text{cm}^2/\text{hr}$  respectively. In our experiments, transdermal flux values for atenolol following the use of silicon, stainless steel microneedles as well as microneedle skin roller were  $2.35 \pm 0.49$ -,  $2.62 \pm 0.59$ - and  $1.65 \pm 0.33 \text{ ng}/\text{cm}^2/\text{hr}$  respectively. Transcutaneous flux values for bisoprolol following the use of silicon and stainless steel microneedles were  $2.79$ - and  $2.31 \mu\text{g}/\text{cm}^2/\text{hr}$  respectively. Twelve passes of a gold-titanium microneedle skin roller resulted in a transdermal flux of  $3.44 \mu\text{g}/\text{cm}^2/\text{hr}$ .

## DISCUSSION

Many beta-blockers are limited in their ability to reach systemic circulation following transdermal administration. This is due to their hydrophilicity and the excellent barrier properties of the stratum corneum. Anroop et al. 2009<sup>27</sup> and Modamio et al., 2000<sup>20</sup> reported passive flux values values of  $0.55 \mu\text{mol}/\text{cm}^2$  and  $1.19 \mu\text{g cm}^2/\text{h}$  for atenolol and bisoprolol respectively. Zhao et al. (2007)<sup>23</sup> investigated the synergistic effect of isosorbide dinitrate on percutaneous penetration of bisoprolol. Anroop et al. studied transdermal iontophoretic delivery of atenolol prodrugs across porcine skin. Flux value for atenolol valerate using iontophoresis was  $1.48 \mu\text{mol}/\text{cm}^2$ . Puglia and Bonina, 2008<sup>22</sup> also studied the effect of polyunsaturated fatty acids (chemical penetration enhancers) on percutaneous penetration of atenolol.

Chemical penetration enhancers (CPE) have also been used to increase transdermal flux of insulin.<sup>28</sup> In spite of widespread evaluation of chemical penetration enhancers for transdermal drug delivery, none is ideal. CPE are usually not effective in delivering hydrophilic molecules.<sup>29,30</sup> Williams and Barry have also noted that it is difficult to rationally select a penetration enhancer for a given permeant since enhancer potencies are drug specific. Also, even though numerous chemical penetration enhancers (CPEs) have been investigated for transdermal drug delivery, their toxic effects limit their use in transdermal patches. The degree of effectiveness of CPEs is usually accompanied by an increase in their toxic effects because potential CPEs are known to irritate and disrupt the organized structure of the skin.<sup>31</sup>

Our study sought to overcome these limitations by employing a different approach-the use of microneedles.

Microneedles can bypass the stratum corneum and enhance transdermal delivery by creating transient aqueous pathways of micron dimensions.<sup>32</sup>

For a drug to be effective in transdermal drug delivery, it must cross the stratum corneum, viable epidermis and dermis. *In vitro* studies usually investigate the effect of microneedle factors on percutaneous penetration. These factors include microneedle density, microneedle length, insertion force and insertion time. Other factors that can influence transdermal drug delivery include the characteristics of created microconduits and molecular properties of the drug.<sup>33</sup> In most cases, increase in microneedle length leads to enhancement in transdermal flux although this does not always hold. The same observation generally applies to microneedle density-a higher microneedle density positively correlates with increase in transdermal drug delivery.

These needles can be made from a wide range of materials (metals, silicon, polymers) and they can have different shapes (pyramidal, cylindrical, quadrangular, etc.). Li et al.<sup>34</sup> used maltose and metal microneedles to enhance the transdermal delivery of human immunoglobulin G across hairless rat skin. In that study, the authors evaluated microneedles made from different materials. Wermeling et al.<sup>35</sup> used microneedles to enhance transdermal delivery of a skin-impermeant molecule, naltrexone in humans. While passive penetration did not result in plasma concentration, the use of microneedles resulted in the plasma detection of the drug within two hours.

Digital images of silicon, stainless steel microneedles are shown in Figures 1 and 2 respectively. Figure 3 is a digital image of gold-titanium microneedle roller. Percutaneous experiments across porcine ear skin were carried out to determine enhancement of skin permeability by silicon, stainless steel microneedles as well as gold-titanium microneedle roller. Microneedles with various depths ( $200 \mu\text{m}$  and  $500 \mu\text{m}$ ) were used to enhance skin penetration of atenolol and bisoprolol hemifumarate. For atenolol, the highest penetration was obtained with stainless steel microneedles. Flux was 2.2 fold compared with passive penetration. Gold-titanium microneedle roller also increased transdermal flux of bisoprolol hemifumarate. This is a handheld device with gold-titanium microneedles embedded in the head. This device with a density of 192 microneedles was used to microporate pig ear skin. The microchannels in the skin formed by rolling the microneedle roller across the skin are comparable to those created by stainless steel microneedles.

Microneedle rollers are useful in the treatment of large skin areas. In this scenario, microneedles are mounted on a cylindrical surface and can be rolled across the skin, such that each microneedle is able to pierce the skin many times as the roller moves across the skin. When this device was used in our experiments, there was a 2.94-fold increase in transcutaneous flux for bisoprolol hemifumarate in comparison with passive diffusion across porcine

ear skin. Transcutaneous flux is a complex phenomenon that depends not only on microneedle geometry but also on the physicochemical properties of the permeant. It is possible that although theoretically, a higher microneedle density of the roller should result in a higher flux, other factors relating to the complex interaction between the skin and the drug may play a significant role leading to the observed higher flux of atenolol from stainless steel microneedle-pretreated skin compared to gold-titanium roller. In summary, the results of our studies with silicon, stainless steel microneedles as well as gold-titanium microneedle rollers indicate that these devices can create microchannels in the skin and enhance *in vitro* transport of atenolol and bisoprolol hemifumarate.

## CONCLUSION

Microneedle-mediated transdermal drug delivery can lead to increased patient compliance because of their simplicity and ease of use. This is especially important in the delivery of therapeutic agents used in the treatment of chronic diseases such as hypertension. In our study, microneedles disrupted the stratum corneum of pig ear skin and significantly enhanced percutaneous penetration of atenolol and bisoprolol hemifumarate. The effectiveness of this approach was demonstrated by increased diffusion of atenolol and bisoprolol hemifumarate across porcine ear skin as determined by liquid chromatography-mass spectrometry. By using microneedles, it may be feasible to develop transdermal patches for these drugs.

**Acknowledgment:** The authors are grateful to Touro University, California for financial support. We also thank Monika Kaur for assistance with digital images.

## REFERENCES

1. H. B. Bosworth, M. K. Olsen, T. Dudley, M. Orr, A. Neary, M. Harrelson, M. Adams, L. P. Svetkey, R. J. Dolor, and E. Z. Oddone, The take control of your blood pressure (TCYB) study: Study design and methodology. *Contemporary Clinical Trials* 28, 33 (2007).
2. World Health Report 2002: Reducing Risks, Promoting Healthy Life. Geneva, Switzerland: World Health Organization. <http://www.who.int/whr/2002/>.
3. S. L. Rywyk, C. E. Davis, A. Pajak, G. Broda, A. R. Folsom, E. Kawalec, and O. D. Williams, Poland and U.S. collaborative study on cardiovascular epidemiology hypertension in the community: Prevalence, awareness, treatment and control of hypertension in the pol-MONICA project and the U.S. atherosclerosis risk in communities study. *Annals of Epidemiology* 8, 3 (1998).
4. M. Milewski, T. R. Yerramreddy, P. Ghosh, P. A. Crooks, and A. L. Stinchcomb, *In vitro* permeation of a pegylated naltrexone prodrug across microneedle-treated skin. *J. Control Rel.* 146, 37 (2010).
5. K. B. Ita, J. Du Preez, M. E. Lane, J. Hadgraft, and J. du Plessis, Dermal delivery of selected hydrophilic drugs from elastic liposomes: Effect of phospholipid formulation and surfactants. *J. Pharm Pharmacol.* 59, 1215 (2007).
6. M. Sabitha, N. Sanoj Rejinold, A. Nair, V.-K. Lakshmanan, S. V. Nair, and R. Jayakumar, Curcumin loaded chitin nanogels for skin cancer treatment via the transdermal route. *Nanoscale* 4, 239 (2012).
7. M. Sabitha, N. Sanoj Rejinold, A. Nair, V.-K. Lakshmanan, S. V. Nair, and R. Jayakumar, Development and evaluation of 5-fluorouracil loaded chitin nanogels for treatment of skin cancer. *Carbohydrate Polymers* 91, 48 (2013).
8. X. Chen, D. Shah, G. Kositrana, D. Manstein, R. R. Anderson, and M. X. Wu, Facilitation of transcutaneous drug delivery and vaccine immunization by a safe laser technology. *J. Control Rel.* [Epub ahead of print] (2012).
9. K. B. Ita and A. K. Banga, *In vitro* transdermal iontophoretic delivery of penbutolol sulfate. *Drug Deliv.* 16, 11 (2009).
10. R. Yamamoto, S. Takasuga, Y. Yoshida, S. Mafune, K. Kominami, C. Sutoh, Y. Kato, M. Ito, M. Yamauchi, K. Kanamura, and M. Kinoshita, *In vitro* and *in vivo* transdermal iontophoretic delivery of naloxone, an opioid antagonist. *Int. J. Pharm.* 422, 132 (2012).
11. B. E. Polat, D. Hart, R. Langer, and D. Blankschtein, Ultrasound-mediated transdermal drug delivery: Mechanisms, scope, and emerging trends. *J. Control Rel.* 152, 330 (2011).
12. A. Herwadkar, V. Sachdeva, L. F. Taylor, H. Silver, and A. K. Banga, Low frequency sonophoresis mediated transdermal and intradermal delivery of ketoprofen. *Int. J. Pharm.* 423, 289 (2012).
13. J. Choi, M. K. Choi, S. Chong, S. J. Chung, C. K. Shim, and D. D. Kim, Effect of fatty acids on the transdermal delivery of donepezil: *In vitro* and *in vivo* evaluation. *Int. J. Pharm.* 422, 83 (2012).
14. S. M. Bal, A. C. Kruithof, R. Zwier, E. Dietz, J. A. Bouwstra, J. Lademann, and M. C. Meinke, Influence of microneedle shape on the transport of a fluorescent dye into human skin *in vivo*. *J. Control Rel.* 147, 218 (2010).
15. L. Y. Chu and M. R. Prausnitz, Separable arrowhead microneedles. *J. Control Rel.* 149, 242 (2011).
16. A. C. R. Grayson, R. S. Shawgo, L. Yi, and M. J. Cima, Electronic MEMS for triggered delivery. *Adv. Drug Deliv. Rev.* 56, 173 (2004).
17. P. C. Demuth, X. Su, R. E. Samuel, P. T. Hammond, and D. J. Irvine, Nano-layered microneedles for transcutaneous delivery of polymer nanoparticles and plasmid DNA. *Adv. Mater.* 43, 4851 (2010).
18. C. P. Zhou, Y. L. Liu, H. L. Wang, P. X. Zhang, and J. L. Zhang, Transdermal delivery of insulin using microneedle rollers *in vivo*. *Int. J. Pharm.* 392, 127 (2010).
19. Y. C. Kim, J. H. Park, and M. R. Prausnitz, Microneedles. *Adv. Drug Deliv. Rev.* (Eprint ahead of print) (2012).
20. P. Modamio, C. F. Lastra, and E. L. Mariño, A comparative *in vitro* study of percutaneous penetration of beta-blockers in human skin. 194, 249 (2000).
21. P. Modamio, C. F. Lastra, and E. L. Mariño, Transdermal absorption of celiprolol and bisoprolol in human skin *in vitro*. *Int. J. Pharm.* 173, 141 (1998).
22. C. Puglia and F. Bonina, Effect of polyunsaturated fatty acids and some conventional penetration enhancers on transdermal delivery of atenolol. *Drug Delivery* 15, 107 (2008).
23. J. Zhao, J. Fu, S. Wang, C. Su, Y. Shan, S. Kong, Y. Wang, W. Lu, H. Zhang, S. Zhang, L. Li, E. Zhang, L. Wang, Q. Pei, J. Wang, X. Zhang, and Q. Zhang, A novel transdermal patch incorporating isosorbide dinitrate with bisoprolol: *In vitro* and *in vivo* characterization. *Int. J. Pharm.* 337, 88 (2007).
24. W. Meyer, J. Kacza, N. H. Zschemisch, S. Godynicki, and J. Seeger, Observations on the actual structural conditions in the stratum superficiale dermidis of porcine ear skin, with special reference to its use as model for human skin. *Ann. Anat.* 189, 143 (2007).
25. V. Klang, J. C. Schwarz, B. Lenobel, M. Nadj, J. Auböck, M. Wolzt, C. Valenta, *In vitro* versus *in vivo* tape stripping: Validation of the porcine ear model and penetration assessment of novel sucrose stearate emulsions. *Eur. J. Pharm. Biopharm.* 80, 604 (2012).
26. B. Chen, J. Wei, and C. Iliescu, Sonophoretic enhanced microneedles array (SEMA)—Improving the efficiency of transdermal drug delivery. *Sensors and Actuators B: Chemical* 145, 54 (2010).
27. B. Anroop, B. Gosh, V. Parcha, and J. Khanam, Transdermal delivery of atenolol: Effect of prodrugs and iontophoresis. *Curr. Drug Deliv.* 6, 280 (2009).

28. K. M. Yerramsetty, B. J. Neely, S. V. Madihally, and K. A. M. Gasem, A skin permeability model of insulin in the presence of chemical penetration enhancer. *Int. J. Pharm.* 388, 13 (2010).
29. A. C. Williams and B. W. Barry, Penetration enhancers. *Adv. Drug Del. Rev.* 64, 128 (2012).
30. K. Brychtova, L. Dvorakova, R. Opatrilova, I. Raich, S. Kacerova, L. Placek, D. S. Kalinowski, D. R. Richardson, and J. Jampilek, Investigation of substituted 6-aminohexanoates as skin penetration enhancers. *Bioorganic and Medicinal Chemistry* 20, 86 (2012).
31. B. W. Barry, Novel mechanisms and devices to enable successful transdermal drug delivery. *Eur. J. Pharm. Sci.* 14, 101 (2001).
32. R. F. Donnelly, T. R. Raj Singh, and A. D. Woolfson, Microneedle-based drug delivery systems: Microfabrication, drug delivery, and safety drug delivery, *Drug Deliv.* 17, 187 (2010).
33. Y. A. Gomaa, M. J. Garland, F. J. McInnes, R. F. Donnelly, L. K. El-Khordagui, and C. G. Wilson, Flux of ionic dyes across microneedle-treated skin: Effect of molecular characteristics. *Int. J. Pharm.* 438, 140 (2012).
34. G. Li, A. Badkar, H. Kalluri, and A. K. Banga, Microchannels created by sugar and metal microneedles: Characterization by microscopy, macromolecular flux and other techniques. *J. Pharm. Sci.* 99, 1931 (2010).
35. D. P. Wermeling S. L. Banks, D. A. Hudson, H. S. Gill J. Gupta, M. R. Prausnitz, A. L. Stinchcomb, Microneedles permit transdermal delivery of a skin-impermeant medication to humans. *Proc. Natl. Acad. Sci. USA* 105, 2058 (2008).